

**EXPERIMENTAL AND NUMERICAL STUDIES OF  
DISPLACEMENT FIELDS AND FAILURE MECHANISMS  
IN UNTREATED AND REINFORCED SLOPES USING  
DIGITAL IMAGE DISPLACEMENT (DID)**

by

Gael Araujo

Submitted in Partial Fulfillment  
of the Requirements for the Degree of  
Master of Science in Mineral Engineering with  
Specialization in Geotechnical and Geomechanical Engineering



New Mexico Institute of Mining and Technology  
Socorro, New Mexico  
December, 2024

This thesis is dedicated to all those passionate about landslides and image processing.

Gael Araujo  
*New Mexico Institute of Mining and Technology*  
*December, 2024*

## ABSTRACT

Slope failures have led to devastating human casualties and significant economic losses worldwide, with annual impacts estimated at US\$ 4.5 billion in Japan, US\$ 2.6 billion in Italy, US\$ 2 billion in the United States, and US\$ 1.5 billion in India [1], [2], [3]. This highlights the critical importance of slope stability analysis, which focuses on understanding potential failure shapes and their associated displacement fields. The mining industry is familiar with this risk; as large-scale mining operations generate more waste stored in tailings dams with a history of catastrophic failures. Notable incidents include the Buffalo Creek disaster (1972), the Baia Mare spill (2000), and the Brumadinho disaster (2019), resulting in substantial fatalities and environmental damage. These events underscore the urgent need for effective slope stability analysis and a deeper understanding of slope behavior to reduce or mitigate the associated risks.

This study pioneers the application of image processing techniques for analyzing displacement fields and failure surfaces of slopes subjected to induced loads. Introducing the Digital Image Displacement (DID) method enhances the visualization and identification of critical failure surfaces, thus deepening our understanding of slope behavior. The methodology was further refined using MATLAB for data correction and rescaling, alongside numerical verification through the Finite Element Method (FEM) via Plaxis 3D and safety factor calculations using the Limit Equilibrium Method (LEM) with Slide2 software.

In this study, over 40 experiments were conducted, analyzing more than 700 digital images to investigate the failure shapes and displacement fields of untreated and geogrid-reinforced sandy slopes. The aim was to gain insights into soil behavior and its response to reinforcement under load. Direct shear tests revealed a friction angle of  $37^\circ$  for the sand, leading to the selection of slope angles between  $30^\circ$  and  $35^\circ$  for the experiments.

The experimental setup evolved through three stages. Initially, a basic acrylic box measuring  $50\text{ cm} \times 35\text{ cm} \times 9\text{ cm}$  (L×W×T) was used, which was later upgraded to a more robust polycarbonate box measuring  $55\text{ cm} \times 30\text{ cm} \times 10\text{ cm}$  (L×W×T), and finally, the same polycarbonate including a loading frame for precise load application. The slope was manually loaded in stages 1 and 2 using dead loads, while in stage 3, automatic loading was implemented. Each load increment at the top of the slope, from its static to its failure states, was documented with photographs to capture the process.

Experiments in Stage 3 yielded more reliable results due to the automatic load application provided by the Versa loading frame, which performed uniaxial compression tests alongside a stronger frame box. For untreated slopes at  $30^\circ$  and  $35^\circ$  angles, maximum load capacities ranged from 679 N to 736 N and 598 N to 628 N, respectively. Displacement at failure ranged from 4.05 to 4.8 mm for the  $30^\circ$  slope and 4.75 to 4.9 mm for the  $35^\circ$  slope. These results closely aligned with PLAXIS 3D

simulations, confirming the reliability of the experimental setup. In contrast, the reinforced slopes demonstrated significantly enhanced stability, with maximum loads ranging from 1250 N to 1700 N. Total displacements for the reinforced slopes were 6.2 mm to 7.1 mm, with load capacities ranging from 929 N to 1171 N for the 30° and 35° angles, respectively. Total displacements were between 5.1 mm and 7.0 mm for different geogrid spacings, including one-half, two-fifths, and one-third spacing. Load normalization showed that decreasing geogrid spacing improved load-bearing capacity and overall stability, with one-third spacing being the most effective.

The analysis revealed a logarithmic spiral shape for both untreated and reinforced slopes; however, the reinforced slopes exhibited deeper and more pronounced rupture surfaces. This indicates that they can withstand higher loads before experiencing significant deformation. Geogrid reinforcement has been shown to enhance slope stability significantly. Still, a comprehensive assessment of slope geometry and compaction is essential, as these factors can dramatically influence overall stability, either enhancing or diminishing it.

This study improves the precision of displacement measurements and provides valuable insights into the mechanisms of slope failure, which are critical for developing effective risk mitigation strategies. The findings could significantly advance the field of geotechnical engineering by establishing new standards for analyzing slope stability.

**Keywords:** Slope failure; Digital Image Displacement; Geogrid reinforcement; Logarithmic spiral; Compaction.

## ACKNOWLEDGMENTS

I would like to extend my deepest gratitude to Dr. Navid for accepting me as a new student in the Mineral Engineering program at New Mexico Tech. From our first conversation about my interest in pursuing a master's degree, he provided helpful guidance that made the process easier. His support and the provided funding were essential in helping me complete my academic studies.

I am also profoundly grateful to Dr. Mehrdad Razavi for his guidance and dedication at every stage of this research. Thank you for your involvement and commitment, including the many hours we spent building the polycarbonate wooden box and for patiently addressing all my questions. I truly appreciate the opportunity to be your student.

I sincerely thanks Dr. Wilson for her unwavering support and commitment to my project. Without hesitation, she agreed to be a part of my committee, offering valuable guidance and encouragement throughout the process.

My heartfelt thanks go to my boyfriend, Jose Raul Zela. Five years ago, I never imagined I could continue doing what I love—working with landslides in another industry that is not research. Raul encouraged me to pursue a path in the mining industry, and while I am just beginning, I am confident that I will deepen my knowledge from this perspective. I appreciate the countless hours he spent with me in the laboratory, assisting with my experiments. His unwavering support, patience, and understanding have motivated me during the most challenging times. This work would not have been possible without him.

I would like to express my gratitude to Dr. Mostafa Hassanalian, whose support was instrumental in the successful mechanical setup of the loading frames. Dr. Hassanalian not only provided all the necessary materials but also demonstrated a strong willingness to assist throughout the process. His availability and eagerness to help were evident, and I am especially grateful for his generosity in allowing his student, Logan Moore, to contribute to the mechanical setup of the loading frames. Progressing through the experimental stages was only possible without their expertise and hands-on assistance in making critical mechanical adjustments to the Versa loader frames.

Special thanks to Peter Lyons and Alfredo Romero for their crucial help with acrylic cuts and the manual load application, which was essential for successfully executing the first and second stages of the experiment. I also extend my gratitude to Golfred Amponsah, a former Mineral Engineering Department student, who constructed an acrylic box I used in the first stage of my experiments. Thank you for providing this equipment.

Finally, I would like to thank my family for their unwavering support from a distance, for their constant encouragement, and for caring for my plants.

# CONTENTS

ABSTRACT	
ACKNOWLEDGMENTS .....	v
LIST OF TABLES .....	ix
LIST OF FIGURES .....	x
LIST OF ABBREVIATIONS AND SYMBOLS.....	xii
<b>CHAPTER 1</b> .....	1
1.1 Introduction .....	1
1.2 Problem Statements .....	3
1.3 Objectives .....	3
1.4 Research questions that guide the investigation .....	4
1.5 Significance of the Study .....	4
1.6 Challenges .....	5
<b>CHAPTER 2</b> .....	6
LITERATURE REVIEW .....	6
2.0 Introduction .....	6
2.1 Failure Surface in a Slope .....	6
2.2 Method for Identifying Surface Failure Shapes and Critical Areas .....	7
2.3 Effect of Geogrid on Slope Stability .....	10
2.4 Geogrid and Size Particles .....	10
2.5 Deformation of Reinforced Sand under Load .....	14
2.6 Stability Analysis Methods of Reinforced and Unreinforced Slopes.....	14
2.7 Digital Image Correlation (DIC) and Applications in Geotechnics .....	17
2.7.1 Applications in Experimental Geotechnics .....	17
2.7.2 Innovations in Modeling and Simulation .....	17
2.7.3 Technological Advancements and Future Directions .....	19
2.8 Mathematica and Matlab for Image Processing .....	20
<b>CHAPTER 3</b> .....	21
SOIL PROPERTIES, TESTING APPROACHES, AND INSTRUMENTATION.....	21
3.1 Soil Properties – Laboratory tests .....	21
3.1.1 Grain Size Distribution (GSD) Test. ....	21
3.1.2 Direct Shear Test.....	22

	- Direct Shear Test of Coarse Sand Particles.....	22
	- Direct Shear Test of the interface between Coarse Sand and Geogrid .....	24
3.2	Instrumentation Materials.....	25
	<b>CHAPTER 4</b> .....	27
	DATA ACQUISITION AND METHODOLOGY .....	27
4.1	Strategy.....	27
4.2	Data Acquisition.....	27
	4.2.1 Evolution of the experiment instrumentation setup .....	27
	- Stage 1 .....	27
	- Stage 2 .....	27
	- Stage 3 .....	28
	4.2.2 Laboratory experiments procedure.....	28
	- Stages 1 and 2.....	28
	- Stage 3 .....	29
	4.2.3 Data .....	30
4.3	Methodology .....	30
	4.3.1 Image Cropping.....	30
	4.3.2 Digital Image Displacement Method (DID).....	31
	4.3.3 Finite Element Method (FEM).....	31
	4.3.4 Limit Equilibrium Method (LEM) .....	32
	<b>CHAPTER 5</b> .....	33
	RESULTS AND DISCUSSION .....	33
5.1	Results .....	33
	5.1.1 Untreated Slope Analysis .....	33
	- Uniaxial Compression test results for untreated slopes (stage 3 of the experiment setup). .....	33
	- Results of Digital Image Displacement (DID).....	35
	5.1.2 Reinforced Slope Analysis .....	38
	- Uniaxial Compression test for reinforced slope (stage 3 of the experiment setup) .....	38
	- Results of Digital Image Displacement (DID).....	40
	5.1.3 Plaxis 3D Simulation with the same load.....	46
5.2	Discussion .....	50
	5.2.1 Relationship between the maximum load supported in untreated and reinforced slopes.....	50
	5.2.2 Displacement fields under untreated and reinforced slopes .....	51
	5.2.3 Failure Shape of Untreated and Reinforced Slope .....	52
	5.2.5 Additional Observations:.....	55
	5.2.4 Factor of Safety Calculation.....	55

5.2.5 Additional Observations.....	55
- Compaction effect on loading support .....	55
<b>CONCLUSIONS</b> .....	56
<b>RECOMMENDATIONS</b> .....	57
<b>REFERENCES</b> .....	58
APPENDIX A .....	62
APPENDIX B.....	64
APPENDIX C.....	70
APPENDIX D .....	85
Permissions for Figures:.....	85

PREVIEW

## LIST OF TABLES

<i>Table 1. Summary of untreated slope failure characteristics .....</i>	35
<i>Table 2. Summary of reinforced slope failure data with instrumentation setup.....</i>	41
<i>Table 3. Maximum displacement fields comparison between DID and PLAXIS 3D .....</i>	46
<i>Table 4. Displacement fields in untreated and reinforced slopes.....</i>	46

PREVIEW

## LIST OF FIGURES

<i>Figure 2.1: Types of slope failure. a) Base slide. b) Toe slide, and c) Slope slide [22]. ....</i>	7
<i>Figure 2.2: Comparison of sliding surface position by different methods, unit in m [4]. ...</i>	8
<i>Figure 2.3: Factor of Safety comparison by Genetic Algorithm (GA), Monte-Carlo, and Grid methods [10]. .....</i>	9
<i>Figure 2.4: Relationship between shearing strength versus shear displacement in soil particles and geogrid. a) Normal stress 50kPa. b) Normal stress 100 kPa [14]. .....</i>	11
<i>Figure 2.5: Failure Surface of unreinforced slope. a,b) <math>D = 0</math>. c,d) <math>D=B</math> and e,f) <math>D = 2B</math> [30]. .....</i>	13
<i>Figure 2.6: Failure Surface of a reinforced slope. a, b) <math>L = 2B</math>. c, d) <math>L = 4B</math> and e, f) <math>L = 6B</math>, all edges distance <math>D=1B</math> [30]. .....</i>	13
<i>Figure 2.7: Comparison of a deterministic factor of safety values and failure modes for reinforced slopes. a) using FEM and LEM, b) deformed mesh, c) LEM (Bishop's Simplified Method) [14]. .....</i>	15
<i>Figure 2.8: a) Variation in FS with cohesion. b) Variation in FS with internal friction angle (<math>\phi</math>) [29]. .....</i>	17
<i>Figure 2.9: Camera inclination. a) <math>\theta = 0^\circ</math>, b) <math>\theta = 21.5^\circ</math> [34]. .....</i>	18
<i>Figure 2.10: Measurement of incremental subset displacement with DIC [33]. .....</i>	19
<i>Photography 1. GSD of the soil. Sieves N° 20 (499 gr) and N° 60 (1 gr) .....</i>	21
<i>Photography 2. Direct shear test of coarse sand. ....</i>	22
<i>Figure 3.1: Shear stress vs. horizontal displacement for a vertical load of 3600N, 1200N, and 400N from top to bottom. ....</i>	23
<i>Figure 3.2: Normal stress vs Shear stress .....</i>	23
<i>Figure 3.3: Set up of the shear box for sand and geogrid [11] .....</i>	24
<i>Figure 3.4: Shear stress vs displacement curve of sand and sand/geogrid. ....</i>	24
<i>Figure 3.5: Instrumentation Materials .....</i>	26
<i>Figure 4.1: Stage in the Evolution of the Instrumentation Setup .....</i>	28
<i>Figure 4.2: Laboratory Experimental Procedure .....</i>	29
<i>Figure 4.3: Photograph acquisition in the laboratory experiments .....</i>	30
<i>Figure 4.4.: Methodology flow and structure .....</i>	32
<i>Figure 5.1: Force versus vertical displacement in untreated 30° slopes. ....</i>	34
<i>Figure 5.2: Force versus vertical displacement in untreated 35° slopes. ....</i>	34
<i>Figure 5.3: Displacement fields evolution of Untreated 30° slope with DID method. ....</i>	36
<i>Figure 5.4: Displacement fields evolution of Untreated 30° slope with DID method. ....</i>	37

<i>Figure 5.5: View of displacement fields in PLAXIS 3D simulation of untreated slope with 30° and 35°.</i>	38
<i>Figure 5.6: Load application in a compression test to Reinforced 30° and 35° slopes, with one-third (1/3), two-fifth (2/5) and one-half (1/2) spacing.</i>	39
<i>Figure 5.7: Geogrid spacing configuration.</i>	41
<i>Figure 5.8: Displacement fields evolution of Reinforced 30° slope with one-third spacing, using DID method.</i>	42
<i>Figure 5.9: Displacement fields evolution of Reinforced 30° slope with two-fifth spacing, using DID method.</i>	43
<i>Figure 5.10: Displacement fields evolution of Reinforced 35° slope with one-third spacing, using DID method.</i>	44
<i>Figure 5.11: Displacement fields evolution of Reinforced 35° slope with two-fifth spacing (test 1), using DID method.</i>	45
<i>Figure 5.12: Displacement fields under untreated and reinforced slopes at 1630N – 30°.</i>	47
<i>Figure 5.13: Factor of safety under untreated and reinforced slopes at 710 N – 30°.</i>	48
<i>Figure 5.14: Measurement Factor of safety under untreated and reinforced slopes at 609N – 35°.</i>	49
<i>Figure 5.15: Maximum load supported under untreated and reinforced condition for 30° and 35° slope angle.</i>	50
<i>Figure 5.16: displacement fields versus force for under untreated and reinforced conditions for 30° and 35° slopes.</i>	51
<i>Figure 5.17: Total displacement correlation under untreated and reinforced slopes at 1630N – 30°.</i>	52
<i>Figure 5.18: Fitting of the rotational and logarithmic spiral surfaces in the DID images that represent the untreated and reinforced slope failure shapes.</i>	53
<i>Figure 5. 19: FS variation with untreated and reinforced condition for 30° and 35° slopes.</i>	54
<i>Figure 5.20: Change of compression curve in four different compaction cases.</i>	55

## LIST OF ABBREVIATIONS AND SYMBOLS

ASTM	American Society for Testing and Materials
B	Width of the scaled plate load
BBO	Biogeography-Based Optimization
CDS	Cyclic Direct Shear
CMUs	Concrete Masonry Units
COV	Coefficients of variation for soil properties
D	Distance from the slope edge
DI	Digital Image
DIC	Digital Image Correlation
DID	Digital Image Displacement
FS	Factor of safety
GA	Genetic Algorithms
GRS	Geosynthetic Reinforced Soil
GSD	Grain Size Distribution
L	Geogrid Length
LEM	Limit Equilibrium Method
MDS	Monotonic Direct Shear
mFEM	Modified Finite Element Method
NMT	New Mexico Tech
P	Vertical Loading
PCDS	Post-Cyclic Direct Shear

PIV	Particle Image Velocimetry
PSO	Particle Swarm Optimization
SRM	Soil-rock mixture
USCS	Unified Soil Classification System

PREVIEW

The dissertation is accepted on behalf of the faculty Institute by the following committee:

Navid Mojtabai

---

Academic Advisor

Merhdad Razavi

---

Research Advisor

Claudia Wilson

---

Committee Member

I release this document to the New Mexico Institute of Mining and Technology.

Gael Estefany Araujo Huaman

November 11, 2024

---

# CHAPTER 1

## GENERAL ASPECTS

### 1.1 Introduction

Slope failure had triggered some of the worst catastrophic scenarios worldwide, causing human casualties and economic losses. For instance, some economic losses associated with slope movements are US\$ 4.5 billion per year in Japan, US\$ 2.6 billion per year in Italy, US\$ 2 billion in the United States, and US\$ 1.5 billion in India [1], [2],[3]. That is why slope stability analysis is essential for mitigating or reducing the risk. The fundamental factors for achieving this include understanding the shape of potential slope failures and assessing displacement field deformations.

Understanding the shape of potential failure surfaces in slope stability analysis is critical. Research has shown that modifying slope geometry by decreasing the slope angle and height can improve stability [4]. Specifically, reducing the slope angle leads to a linear increase in safety, while lowering the slope height results in a parabolic increase in the safety factor. Various failure modes have been identified depending on soil type and slope geometry, such as toe slides in clay and sandy clay at steeper slopes, base slides in shorter slopes, and slope slides in sandy soils [4]. This evidence highlights the importance of accurately characterizing failure surface shapes to enhance slope stability measures.

Traditional methods for identifying failure surfaces often rely on the assumption of a circular shape, which simplifies mathematical and engineering problems. However, recent research has explored alternative shapes, including damped sinusoid, second-degree parabola, and logarithmic spiral, to represent critical slip surfaces more precisely [5]. While these alternative shapes offer greater accuracy, the circular and logarithmic spiral shapes remain widely used [6], [7]. Studies have shown that the spiral surface shape aligns well with the Mohr-Coulomb failure criterion, which aids in the practical modeling of failure surfaces [8]. Advanced methods, such as finite element analysis (FEM-Plaxis 2D), have

revealed that the damped sinusoidal shape better fits critical slope failures compared to circular models. Additionally, mathematical methods like the brachistochrone curve, a cycloid shape, have simplified calculations and enhanced computational efficiency for modeling sliding surfaces [6].

In addressing slope failures, various improvement techniques have been used to reinforce slopes and mitigate slope failures. One of the most popular techniques to enhance slope stability is using geogrids due to their ability to strengthen the soil. Experimental studies, numerical analyses, and finite element methods have demonstrated effectiveness. Geogrids, made from polymers like PET or HDPE [5], are available in various configurations, including unidirectional, bidirectional, and tridirectional forms. Research shows that multidirectional geogrids, particularly those with triangular structures, manage multidirectional loads effectively and improve stability. The characteristics of geogrids, such as tensile strength and elongation, are influenced by factors like temperature changes and tensile rates, with higher tensile rates improving stability [9]. Case studies, such as those in Chandragiri Hill, Nepal, and the Meulaboh–Geumpang landslide in Indonesia, have illustrated the effectiveness of geogrid reinforcement in increasing the factor of safety and improving slope stability [10] [11].

The interaction between geogrids and soil also affects shear strength at the interface. Multidirectional geogrids exhibit higher shear strength than unidirectional and bidirectional types due to transverse ribs enhancing resistance [12], [13], [14]. Although the shear strength at the soil-geogrid interface is generally lower than the soil's inherent shear strength, it is influenced by factors such as soil particle size and density. Studies indicate that larger soil particles and higher sand density improve stability by enhancing adhesion and friction angle [11]. Additionally, research has shown that the vertical spacing of geogrid layers plays a critical role in reinforcing slopes, with increased layer numbers and reduced spacing improving safety factors [15].

Furthermore, advanced methodologies for slope stability analysis now include probabilistic analyses using modified Finite Element Method (mFEM) combined with strength reduction techniques. Research has shown that reinforced slopes exhibit lower failure probabilities than unreinforced slopes, especially with increased variability in soil friction angle [16]. Additionally, new approaches account for lateral swelling in expansive soils by incorporating additional pullout forces and optimizing reinforcement schemes for improved stability [17]. For municipal solid waste (MSW) landfills, optimal geogrid parameters have been found to significantly enhance safety factors, with finite element and limit equilibrium analyses providing detailed insights into failure planes and stress distribution [18].

The interaction between the interface of the soil material and the geogrid was focused on direct shear test analysis and digital image correlation (DIC), a precise optical technique used to measure surface deformations by capturing and analyzing digital images before and after deformation [19], [20]. Recent advancements in DIC technology, including higher-resolution cameras and improved software, have enhanced accuracy and

reduced data processing time [21]. Despite these advancements, few studies have utilized DIC to analyze slope failure shapes directly.

This study uses powerful software like Mathematica and MATLAB to compare failure shapes in geogrid-reinforced versus untreated sandy slopes. By investigating how geogrid reinforcement affects soil behavior and failure surface characteristics, the study seeks to enhance understanding of slope stability and the effectiveness of reinforcement techniques. This research will pioneer the application of Mathematica's Wolfram language in the geotechnical field.

## **1.2 Problem Statements**

Predicting slope stability involves complex challenges, especially when comparing geogrid-reinforced versus untreated sandy slopes. Traditional models for analyzing failure surfaces, such as circular and logarithmic spiral shapes, may only partially capture the slope behavior details. While geogrid reinforcement is expected to be a common technique used to improve stability, its impact on soil behavior and failure surface shape characteristics requires more detailed investigation.

This study uses advanced software tools like Mathematica and MATLAB to perform a comparative analysis of failure shapes in geogrid-reinforced and untreated sandy slopes. The research will enhance our understanding of geotechnical issues by exploring how geogrid reinforcement influences slope stability and failure mechanisms.

## **1.3 Objectives**

1. Investigate the maximum load-bearing capacity of untreated and geogrid-reinforced slopes while analyzing how geogrid spacing configurations influence overall slope stability.
2. Implement Digital Image Displacement (DID) techniques to process, correct, and determine the displacement field of a slope from its static to its failure state for both untreated and reinforced slopes, validating the effectiveness of this method through numerical modeling.
3. Identify and characterize the rupture shapes of untreated and reinforced slopes using DID, focusing on distinguishing features such as circular and logarithmic spiral patterns.

## 1.4 Research questions that guide the investigation

- Are the failure shapes of untreated and geogrid-reinforced slopes similar?
- How can various geogrid configurations affect slope stability, such as layer spacing, and how can these be optimized for sandy soils?
- Why is digital image correlation crucial for understanding slope behavior and failure mechanisms?
- How effective is Mathematica software in digital image processing, and can it be utilized for geotechnical research?
- How can advanced computational tools and methods enhance our understanding of slope failure surface identification?
- Do the results from numerical simulations using Plaxis 3D align with those from laboratory experiments?

## 1.5 Significance of the Study

This study is essential for improving our understanding of slope stability and enhancing engineering practices. It focuses on improving the identification and analysis of slope failure shapes, which is a key for calculating slope stability more accurately. Traditional methods often simplify failure shapes to circular models, which can overlook complex real-world conditions. By experimentally determining failure shapes, this research aims to provide more precise stability predictions, leading to safer and more reliable slope management.

Another critical aspect of the study is the evaluation of geogrids as a reinforcement technique to enhance slope stability. Geogrids are materials used to strengthen soil and prevent slope failures. The research investigates the relationship between the failure shape and the use of geogrids. This exploration can lead to more effective and cost-efficient solutions for slope stabilization, improving safety, and reducing the risk of slope failures.

Additionally, the study introduces the use of Mathematica software for digital image processing in geotechnical research. Mathematica offers advanced capabilities for analyzing digital images and modeling complex slope failure shapes with high precision. This new approach allows for detailed and accurate slope stability assessments, leveraging Mathematica's powerful tools to enhance the analysis of geogrid-reinforced slopes. By integrating this advanced software, the study improves the accuracy of failure shape identification and sets a precedent for using cutting-edge technology in geotechnical engineering.

## 1.6 Challenges

Laboratory Instrumentation and Time Management: The inadequacy of the loading frame size limited testing capabilities in the final stage of the study. To address this issue, a custom mechanical setup was developed, and two existing Versa loaders were reconfigured to ensure successful experiments were conducted. This process took several weeks. The modifications to the loading frames were accomplished with invaluable support from personnel in the Mineral and Mechanical Engineering departments at New Mexico Tech (NMT).

Camera Setup: The camera must be precisely leveled to minimize errors. Ensuring the camera is not inclined helps maintain accuracy and consistency in the captured images, essential for reliable data collection and analysis.

Computational Processing: Processing image correlations in Mathematica requires a powerful workstation for high-resolution images. During the initial stage of the project, the available computer with 48 GB of RAM needed to be increased for this task in Mathematica software. Consequently, the decision was made to export the displacement data from Mathematica and visualize it in MATLAB. Each image-correlation test took 24 hours to export, with each test producing around 310 MB of data. Since each experimental test consists of 17 to 50 photos, the total data size amounts to approximately 5 GB to 152 GB. Facing this computational problem, it was decided to reduce the camera resolution at the project's third stage; this reduced the processing time.

Limited Materials: The geogrid material was limited, but the project goal was still achieved through strategic use. Despite the constraints, carefully managing available materials ensured that the project's progress was not adversely affected.

# CHAPTER 2

## LITERATURE REVIEW

### 2.0 Introduction

Slope failures can lead to human losses, serious social problems, and significant economic losses. Although researchers have studied various aspects of how slopes fail, there are still uncertainties, especially about the slope failure shape, the effective ways to prevent these failures, and the effect of the failure shape in the slope stability analysis. This study will focus on understanding the failure shape of untreated and reinforced slopes under load in dry conditions. Although many methods had been identified and modeled, these failure surfaces beyond traditional circular shapes and image processing techniques were rarely used in geotechnical engineering, especially for detecting failure shapes. Therefore, this chapter will provide a literature review that covers empirical methods for identifying failure shapes, the importance of geogrids as reinforcement materials, and an introduction to image processing as a novel technique for detecting failure shapes in untreated and reinforced slopes. This chapter is divided into eight sections: Slope failure surfaces, methods for identifying surface failure shapes and critical areas, the effect of geogrid on slope stability, geogrid and particle size, deformation of reinforced sand under load, methods for stability analysis of reinforced and unreinforced slopes, digital image correlation (DIC) and applications in geotechnics, and Mathematica and MATLAB for image processing.

### 2.1 Failure Surface in a Slope

While numerous research studies have explained various aspects of slope failure behavior, there remain considerable gaps in our understanding, particularly regarding slope

shape failure and its relation with the factor of safety analysis. Accurately characterizing slope movements is essential for developing effective mitigation strategies [3] and conducting reliable slope stability analyses [5].

Three different types of failure modes (Figure 2.1) were associated with various soil materials and geometries: toe slides occurred in clay and sandy clay at steeper slopes; base slides or slope failures happened in slopes shorter than 2 meters and slope slides, which occur in a portion of the slope, were observed in sandy soils [22].

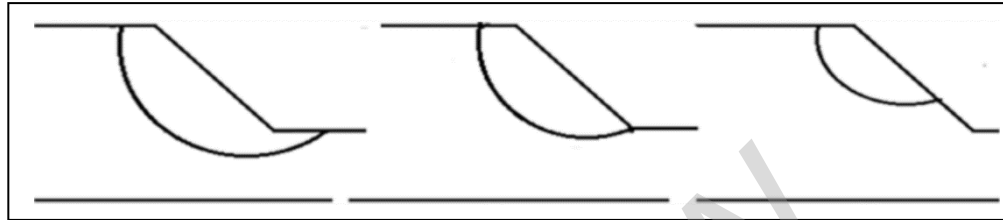


**Figure 2.1: Types of slope failure. a) Base slide. b) Toe slide, and c) Slope slide [22].**  
*Copyright 2019, Springer Nature, unrestricted reprinted.*

Research has shown that a decrease in slope angle and height increases the safety factor, thereby improving slope stability. However, this improvement depends on soil type, slope geometry, and groundwater conditions. Specifically, the analysis indicates that reducing the slope angle results in a linear increase in safety while decreasing the slope height yields a parabolic increase in safety [22].

## **2.2 Method for Identifying Surface Failure Shapes and Critical Areas**

In the literature, many traditional, limit equilibrium, mathematical, physical, seismic, genetic algorithms, numerical, and alternative methodologies have been developed for searching the shape of critical failure surfaces in slopes—all these efforts aimed to improve models to more accurately reflect reality and enhance simulation accuracy. The following sections will explain these methodologies in detail.

Traditional methods assume a circular critical slope failure due to simplifying engineering and mathematic problems. However, recent studies have highlighted alternative shapes, such as a damped sinusoid, second-degree parabola, and logarithmic spiral, to represent the critical slip surface accurately [5]. Despite this amount of surface shape, most studies still use either a circular or logarithmic spiral shape for failure surface analysis. Some researchers compared the stability of embankments by altering the spiral curve shape and found that the spiral surface shape is not determined by the shearing resistance angle (also known as the angle of internal friction), and stability conditions are not significantly affected by the spiral or circular arc surface shapes [23]. While some researchers agree that different assumptions about normal stress on the circular arc of the slip surface lead to only minor differences in stability conditions, they strongly disagree with the conclusion that the angle of shearing resistance does not influence the spiral shape [24].

In the Limit Equilibrium Method (LEM-Slide2) analysis, the shape of the failure is assumed to be circular. This assumption limits the accuracy of modeling the actual slope failure shape. To address this limitation, a finite element method (FEM-Plaxis 2D) was used to evaluate three slope gradients in four regression curves through nonlinear optimization and least-squares fitting. The analysis employed the Mohr-Coulomb criterion to model the shape of the surface failure with high accuracy, as the location and shape were not predetermined before the analysis. The results suggest that the damped sinusoidal shape best fits the critical slope failure [5].

Moreover, mathematical and physical methods have introduced a new sliding surface shape called the brachistochrone. Unlike a straight line or an arc, the brachistochrone is a cycloid (Figure 2.2), which requires two coordinates to draw the curve. This can simplify calculations and reduce computational workload. This study employs the brachistochrone curve to model potential sliding surfaces and calculate the safety factor for multi-level loess slopes using the Janbu method. Improved calculations applied to the brachistochrone curve have led to a new proposed curve that more effectively identifies the most dangerous surfaces with lower safety factors [6].

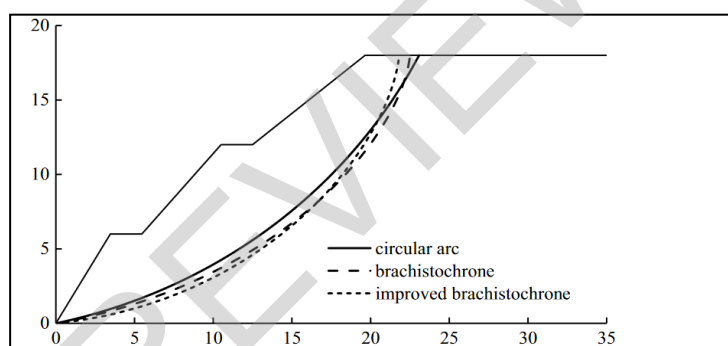


**Figure 2.2: Comparison of sliding surface position by different methods, unit in m [6].**  
**Copyright 2023, Springer Nature, unrestricted reprinted.**

The pseudo-dynamic limit equilibrium method is a seismic analysis that was discussed for the slope failure shape characterization. It represents the phase difference between the primary and shear wave velocities that go through the soil during an earthquake. Its study assumed a log-spiral failure surface shape, a limit, and a moment equilibrium condition for each slide. The seismic acceleration coefficients, slope angles, cohesion, friction angle, slope angle, and surcharge [7], affect the safety factor. Hazari et al. show that the factor of safety decreases as seismic accelerations, slope angle, and surcharge loading increase, while a factor of safety increases as friction angles and cohesion increase. They also concluded that the log-spiral failure surface is more accurate than linear or circular surfaces [7].

Another computationally low-complexity method is the meta-heuristic approach, which is employed to identify critical failure surfaces and determine their safety factors. Singh's et al work on this method explains it through three benchmark case studies [4], each varying in material homogeneity, slope height, angle, layer strength, and water

saturation. The critical failure surfaces for these cases were evaluated using the Fellenius, Bishop, Janbu, and Janbu corrected methods. These methods served as functions for comparing three meta-heuristic algorithms: GA, PSO, and BBO. Among these, the BBO algorithm demonstrated superior accuracy and performance in the factor of safety calculation [4].

Alternative methods were also used to find the critical slip surface and determine the minimum safety factor by refining the trial surface as it approached the critical zone [8], [25]. In contrast, in the Grid method, the critical surface location is found by a square grid of 3 x 3 (9 points) until the center of the grid fits the center of the surface [12], the same that will have a lower factor of safety value. The Monte-Carlo method is comparable to nonlinear programming methods [15]. The limitations of these methods are that they don't guarantee that the critical failure surface is at the global minimum and is simple for particular cases.

Genetic Algorithms (GA) [26] developed for biology have also been optimized to find the critical failure surface, where each potential failure surface represents a chromosome in GA, and its parameters, such as shape and location, are encoded as binary strings. Furthermore, GA uses crossover and mutation operators to refine the failure surface, and adjusting the mutation-crossover probability and population size optimizes slope failure parameters. This method successfully identifies critical slip surfaces in soil slopes, resulting in a lower safety factor than the Grid and Monte-Carlo methods [12] (Figure 2.3).

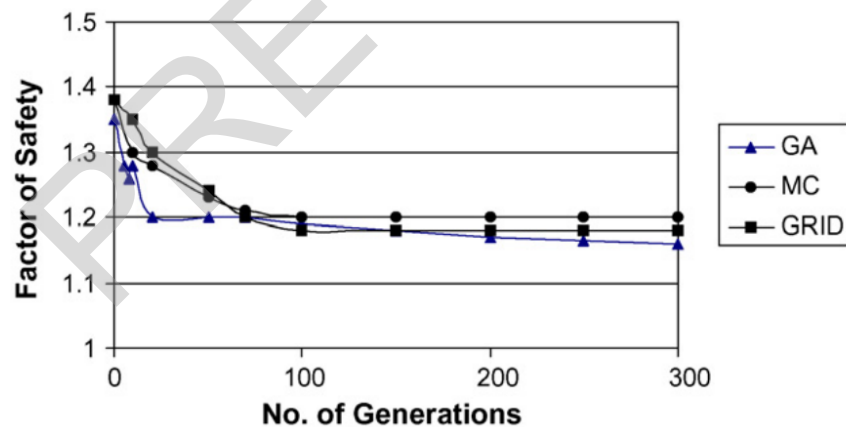


**Figure 2.3: Factor of Safety comparison by Genetic Algorithm (GA), Monte-Carlo, and Grid methods [12]. Copyright 2009, Elsevier, reprinted with permission.**

Many of the methodologies explained above are compared with numerical methods such as PLAXIS 2D and PLAXIS 3D, as these software programs provide results for factor of safety calculations and slope deformation under load, demonstrating their effectiveness. In this study, a pioneering methodology known as Digital Image Displacement will be introduced to identify the critical failure surface visually, and this will also be compared

with PLAXIS 3D to compare the displacement field and, therefore the effectiveness of our work.

### **2.3 Effect of Geogrid on Slope Stability**

Geogrid materials have been widely used to enhance slope stability due to their reinforcement properties. Their efficiency was proven through experimental studies [27], numerical analysis [10], and finite element methods [9]. Geogrids are polymers with various apertures, sizes, and configurations, including unidirectional, bidirectional, and tridirectional forms. They are typically manufactured from PET or HDPE [10].

An experimental analysis investigates the physical properties of a geogrid, load, and time relation [27]. The tests showed that multidirectional geogrids with a triangular structure effectively handle and disperse multidirectional loads, reducing slope failure likelihood. The most important characteristics of a geogrid are its tensile strength and elongation, which temperature changes, grid stretching, and tensile rate can influence. Experimental results show that a higher tensile rate increases tensile strength. Second, multidirectional geogrids enhance slope stability by managing lateral deformation and balancing horizontal thrust with frictional resistance. Third, the load affects creep strain, and low temperatures influence the creep properties of geogrids [27].

A case study in Chandragiri Hill, Kathmandu Valley, Nepal, was selected to address slope stabilization issues [10]. The remediation strategy involved using a geocell wall, geogrid, and micropile anchors to stabilize an unstable slope in a limestone and quaternary area. For the reinforcement, a biaxial square geogrid was chosen. Numerical and conventional analyses of the untreated slope, which had an angle of  $42^\circ$ , indicated a factor of safety of less than 1 using both the Bishop and SSR methods. However, with reinforcement, the factor of safety improved to over 1. This demonstrates that combining these reinforcement techniques effectively mitigates slope failure issues in the Himalayan slopes [10].

Other studies suggest that the vertical spacing of geogrid layers is a significant factor influencing the effectiveness of geosynthetics and, consequently, the slope factor of safety [9]. This was demonstrated through a slope stability analysis of the Meulaboh–Geumpang landslide in Indonesia, using finite element methods under natural and geogrid-reinforced conditions. This analysis adjusted the vertical distance between geogrid layers to reflect the natural slope failure conditions. Under natural conditions, the safety factor is 1.14 and 1.16 in two different sections, indicating a high probability of failure and explaining the landslide occurrence. In contrast, under reinforced conditions, the safety factor ranged from 1.37 to 1.71 and from 1.70 to 2.27 for the two sections, with higher factors of safety achieved as the vertical spacing of the geogrid layers decreased [9].

### **2.4 Geogrid and Size Particles**

The behavior of the geogrid-soil interface revealed that shear strength between the geogrid and soil increases with normal stress [14] [11], [13]. Specifically, multidirectional